ACS Sustainable Chemistry & Engineering

Research Article

pubs.acs.org/journal/ascecg

Murraya koenegii Spreng. Leaf Extract: An Efficient Green Multifunctional Agent for the Controlled Synthesis of Au Nanoparticles

Md N. Alam,[†] Sreeparna Das,[†] Shaikh Batuta,[†] Nayan Roy,[†] Anirban Chatterjee,[†] Debabrata Mandal,[‡] and Naznin A. Begum*[,†]

[†]Department of Chemistry, Visva-Bharati University, Santiniketan 731 235, India

[‡]Department of Chemistry, University College of Science and Technology, University of Calcutta, 92, Acharya Prafulla Chandra Road, Kolkata 700 009, India

Supporting Information

ABSTRACT: There is a demand for the development of reliable, cost-effective, and environment friendly protocols for the synthesis of metal NPs with finely tuned structures for technological applications. In the present work, we have exploited the antioxidant activity of the aqueous extract of dried and pulverized leaves of *Murraya koenigii* Spreng. as a green multifunctional agent in the synthesis of Au NPs with finely tuned morphologies, and our method is a promising green tool for the synthesis of Au NPs with tailor-made structural properties. Moreover, the uniqueness of the present biogenic synthetic route is that simple experimental parameters like control of the concentration of the multifunctional agent and precursor metal ion and also pH and temperature can be effective in the synthesis of Au NPs with finely tuned structures. We have also proposed a plausible mechanistic pathway for our green synthetic route, which may aid in fine-tuning green chemical methods for the controlled synthesis of various metal NPs. At the same time, our study on the interaction between Au NPs and surface-adsorbed fluorescent groups may also be helpful for physicochemical investigations on energy transfer and near-field optical enhancement. Thus, this type of study may be explored in the future for fabricating novel photonic devices.

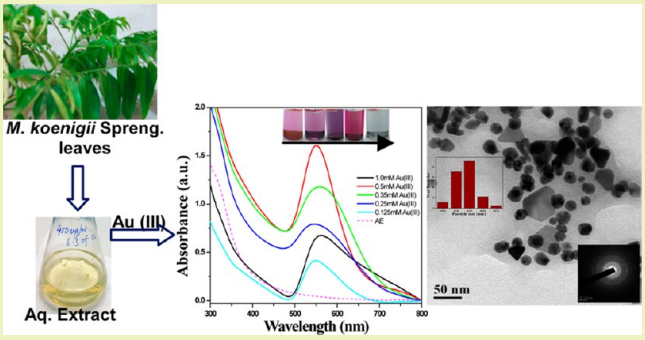

KEYWORDS: *Au NPs, Leaves, Murraya koenigii Spreng., Indian curry leaf plant, Green multifunctional agent, Controlled synthesis*

INTRODUCTION

Gold nanoparticles (Au NPs) have attracted a great deal of attention of various scientific groups in recent years because of their unique catalytic, electronic, optical, and other structure-dependent activities, and subsequent technological applications of Au NPs are being explored extensively.[1] Au NPs also find wide applications in medical science and technology as drug delivery vehicles[2] and fluorescent tags and also as image contrast agents for diagnosis and prevention of cancer.[3,4]Chemical stability and unique optical properties of Au NPs make them ideal candidates for living cell imaging.[1,5] Their performance and hence their applicability depend critically on their size, shape, surface morphology, composition, and fine structure, either as an alloy or core−shell.[6,7]

Hence, the development of energy-efficient, cost-effective, and eco-friendly synthetic routes for Au NPs with tailor-made structural properties and biocompatibility is a very important goal for scientists working in the field of nanoscience and technology. Green Chemistry offers a novel and attractive means to achieve this goal. Over the past few years, in addition to various nontoxic reagents, a plethora of medicinal plants has been explored as green multifunctional agents (GMA) to meet these challenges.[8]

However, in spite of this huge possibility, this stream is still in its infancy. Plant-mediated synthetic protocols for Au NPs reported in the literature so far have been devoted mainly to the production of NPs itself, while little attention has been paid to elucidate the mechanistic pathway. In most of the cases, these methods typically engage the extracts of plant parts that are themselves cocktails of several different compounds. Hence, in most of the reported cases, researchers have failed to identify or even indicate the active component(s) of plant-based GMA. However, such information is indispensable to understand the mechanism of these synthetic routes. This is highly essential for tailor-made and large-scale synthesis of metal NPs. Most of the plant-mediated synthesis procedures of Au NPs have yielded only spherical monometallic NPs.[8] There is still some lacuna in these protocols regarding the enhancement of the functional

Received: September 7, 2013
Revised: February 6, 2014
Published: February 10, 2014

usefulness of synthesized metal NPs by controlling their morphology and composition.

Leaves *of Murraya koenigii* Spreng. (commonly known as Indian curry leaf plant; Fam. Rutaceae) are very rich sources of exogenous antioxidants, for example, flavonoids and polyphenols besides tannic acid and gallic acid.[9] In the present work, we have exploited the antioxidant activity (which indirectly denotes the reducing activity) of an aqueous extract of dried and pulverized leaves of *Murraya koenigii* Spreng. as GMA for the synthesis of Au NPs with finely tuned morphologies. We have also investigated the role of bioprocess parameters like leaf extract and precursor metal [Au (III)] ion concentrations, temperature, and pH on the morphology, aggregation pattern, shape, and size of the NPs] that are essential to enhance the tailor-made structural parameters of the synthesized Au NPs. We also predicted a plausible mechanistic pathway for this green synthetic route of Au NPs that is necessary for standardization, scale-up, and fine-tuning of these types of synthetic methodologies.

Recently, a new direction has been opened toward the synthesis of fluorescent metal NPs using plant-based products.[10] These are particularly relevant in cancer diagnostic techniques, for example, multiple simultaneous profiling of tumor biomarkers and for detection of multiple genes and matrix RNA with fluorescent in situ hybridization.[3,5] So synthesis of biocompatible and fluorescent Au NPs using plant-based multifunctional agents is really an interesting research area that will immensely expand the scope and usefulness of these plant extract-mediated synthetic methods of Au NPs. Fluorescence properties of the Au NP synthesized by our protocol were also studied in detail.

EXPERIMENTAL SECTION

Materials. Chloroauric acid ($HAuCl_4$) (Sigma Aldrich) was used as a source of Au (III) ions required for the synthesis of Au NPs. Folin−Ciocalteu reagent, gallic acid, quercetin ≥95% (HPLC grade), and quercetin-3-glucoside ≥90% (HPLC grade) were purchased from Sigma Aldrich Co. All other chemicals used for the study were of analytical grade and double-distilled deionized water was used for all the analyses.

Instrumentation. Fourier transform-infrared (FT-IR) spectroscopic studies were conducted on a Shimadzu FTIR-8400S PC instrument using KBr pellets in the diffuse reflectance mode. Prior to FT-IR measurements, Au NPs were centrifuged at 12,000 rpm for 20 min followed by drying the samples under vacuum. UV−visible spectroscopy was used to examine the formation and growth of the Au NPs. Absorption spectra were recorded on Shimadzu dual-beam UV−vis-NIR spectrophotometer (model UV PC −3101). Fluorescence spectra of an aqueous solution of GMA, quercetin, quercetin-3-glucoside and the corresponding Au NPs solution synthesized at 50 °C and neutral pH were measured at an excitation wavelength of 300 nm in a Perkin-Elmer LS55 fluorimeter. Water used for spectroscopic studies was triply distilled. All spectroscopic measurements were performed at 25 °C. The spectra of each of the solutions remained unchanged for sufficiently long periods of time during which the spectroscopic experiments were completed. Therefore, any possibility of decomposition of samples that might affect the spectroscopic results can be safely ruled out.

While the absorption spectra provided solid evidence of NPs formation and their growth kinetics, the shape and size of the resultant particles were elucidated with the help of transmission electron microscopy (TEM). Samples for TEM were prepared by drop-coating the Au NPs solution onto carbon-coated copper grids (40 μm × 40 μm mesh size). The films on the grids were allowed to dry prior to the TEM measurement in a JEOL TEM-2010 instrument.

Thermal responses of the Au NPs synthesized by aqueous extract of *Murraya koenigii* Spreng. leaves (AE) was monitored by thermo gravimetric analysis (TGA). TGA of the Au NPs sample was done using a Pyris Diamond TG/DTA (Perkin-Elmer, STA-6000) thermal analyzer. The experiment was set in the temperature range of 40−700 °C and at a heating rate of 10 °C min^{-1} under nitrogen atmosphere.

For powder X-ray diffraction (XRD) analysis, synthesized Au NPs solutions were centrifuged at 14,000 rpm for 30 min, and the supernatant was discarded. Then water was added to the Au NPs and vortexed. Again, the sample was centrifuged in the previous manner. These steps were repeated three times, and finally, the residue part was dried well. The dry powder obtained was spread evenly on a quartz slide to perform X-ray diffraction (XRD) studies. The (XRD) patterns were recorded using the Rigaku Smart Lab diffractometer attached with a D/tex ultra detector and a Cu Kα source operating at 50 mA and 40 kV. The scan range was fixed at 2θ = 10−90° with a stepwise size of 0.02°.

High performance liquid chromatography (HPLC) analyses of the gummy mass obtained from AE (GAE) were done to identify the active biomolecules (polyphenols and polyhydroxy flavonoids) present in this GMA, which are actually responsible for the synthesis and stabilization of Au NPs. Eight milligrams of GAE was dissolved in 20 mL of water (HPLC grade) by sonication for 30 min. After 1 h of standing time, the sample was filtered using Whatman filter paper (0.45 μm), and 10 μL of it was injected in the HPLC column. Similarly, standard solutions of quercetin-3-glucoside (0.075 mM) and quercetin (0.1 mM) in water (HPLC grade) were prepared, and 10 μL of it was injected after filtration by Whatman filter paper (0.45 μm). HPLC analyses were done using Agilent Technologies 1200 Series equipped with an isocratic pump and diode-array detector. The experiment was carried out on Eclipse XDB-C18 (5 μm, 4.6 mm × 150 mm) column (Agilent Technologies, Germany). The mobile phase consisted of methanol:water:formic acid (42:57.5:0.5) (v/v/v). The flow rate was 1.0 mL min^{-1}, and column temperature was 40 °C. Identification of polyhydroxy flavonoids as active components of GMA from HPLC was based on their chromatographic behavior, i.e., according to their retention time. Running time was 30 min, and 360 nm was selected as the detection wavelength for these compounds.

Collection of Leaves of *Murraya koenigii* Spreng. and Its Processing. Leaves were collected from the campus area of Visva Bharati University, Santiniketan, West Bengal, India, during June 2012. Leaves were washed with double-distilled water several times to make it free from dust and then dried under shade. After that, the leaves were pulverized in a mechanical grinder and stored in an airtight container at 4 °C for further use.

Extraction of leaves of *Murraya koenigii* Spreng. At first, 20 g of dried and powdered leaves were macerated in double-distilled deionized water (plant materials:solvent ratio 1:12) at room temperature in a closed container for 24 h with occasional shaking. The extract was then filtered with Whatman No. 42 filter paper to remove any undissolved plant particles. The process was repeated twice using fresh solvent in each time. Finally, the leaves were pressed to get the final extract that was combined with the earlier one. The remaining leaves were then refluxed with 240 mL of double-distilled deionized water for 30 min. This hot aqueous extract was then filtered through Whatman No. 42 filter paper to remove the residual mass and combined with earlier cold extract to get AE. The AE was then lyophilized to dryness, and a gummy mass was obtained. The gummy mass obtained from AE, and GAE was stored at 4 °C and used further as a green multifunctional agent for the controlled synthesis of Au NPs.

Studies on Redox Behavior of AE of *Murraya koenigii* Spreng. Leaves. Cyclic voltammetry (CV) assays for determining the redox behavior of AE were carried out in a potentiostat−galvanostat (PAR Vera Stat TM-II) to explore the electrochemical behavior of the extract. A three-electrode system was employed, viz., SCE as the reference electrode, a platinum wire as a working electrode, and a platinum plate as a counter electrode. The cyclic voltammograms were recorded in the range of −0.7 to +0.9 V with a scan rate of 20 mV s^{-1}.

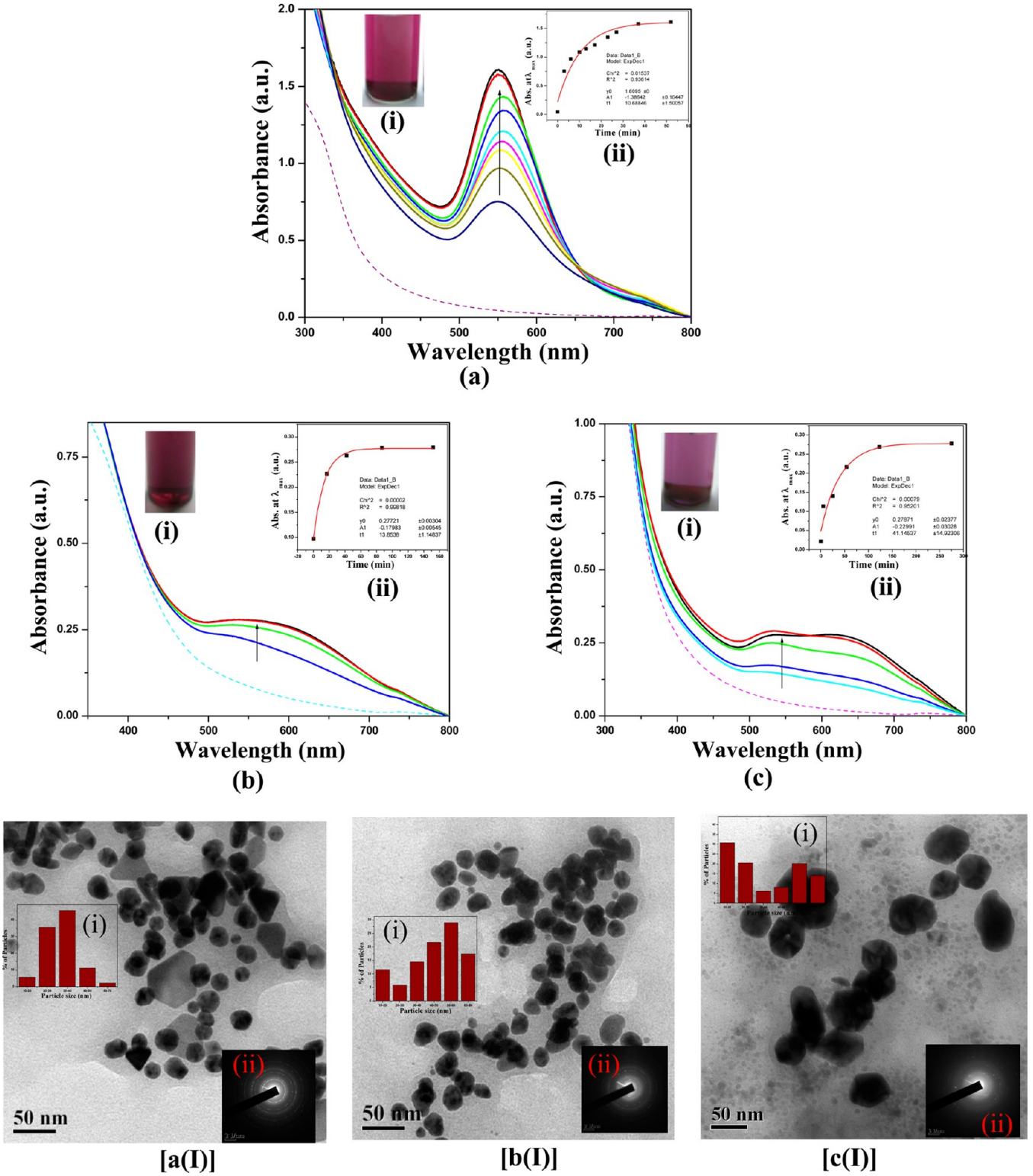

Figure 1. UV−vis spectra of Au NPs prepared by aqueous solution of GAE: (a) 400 μg mL^{-1}, (b) 300 μg mL^{-1}, and (c) 200 μg mL^{-1} at pH 7 and 50 °C. Insets (i) of (a−c) show the color of the corresponding Au NPs solutions after reduction. Insets (ii) of (a−c) show the change in peak absorbance and peak absorption wavelength with time. Broken lines in (a−c) represent the absorbance curves of the reaction medium in the absence of Au (III) ions. TEM images of Au NPs prepared by 400, 300, and 200 μg mL^{-1} aqueous solution of GAE are shown in [a(I)], [b(I)], and [c(I)], respectively. Insets (i) and (ii) of TEM images show the corresponding particle size distribution histograms and SAED patterns of Au NPs, respectively.

Redox behavior of the plant extract is very much dependent on the contents of the reducing species, for example, ploypheno ls and flavonoids, present in it. We have determined total flavonoid and polyphenol contents of AE. The aluminum chloride colorimetric method was used for its total flavonoid content determination,[11] while total polyphenol content of AE was determined colorimetrically by the

dx.doi.org/10.1021/sc400562w | ACS Sustainable Chem. Eng. 2014, 2, 652−664

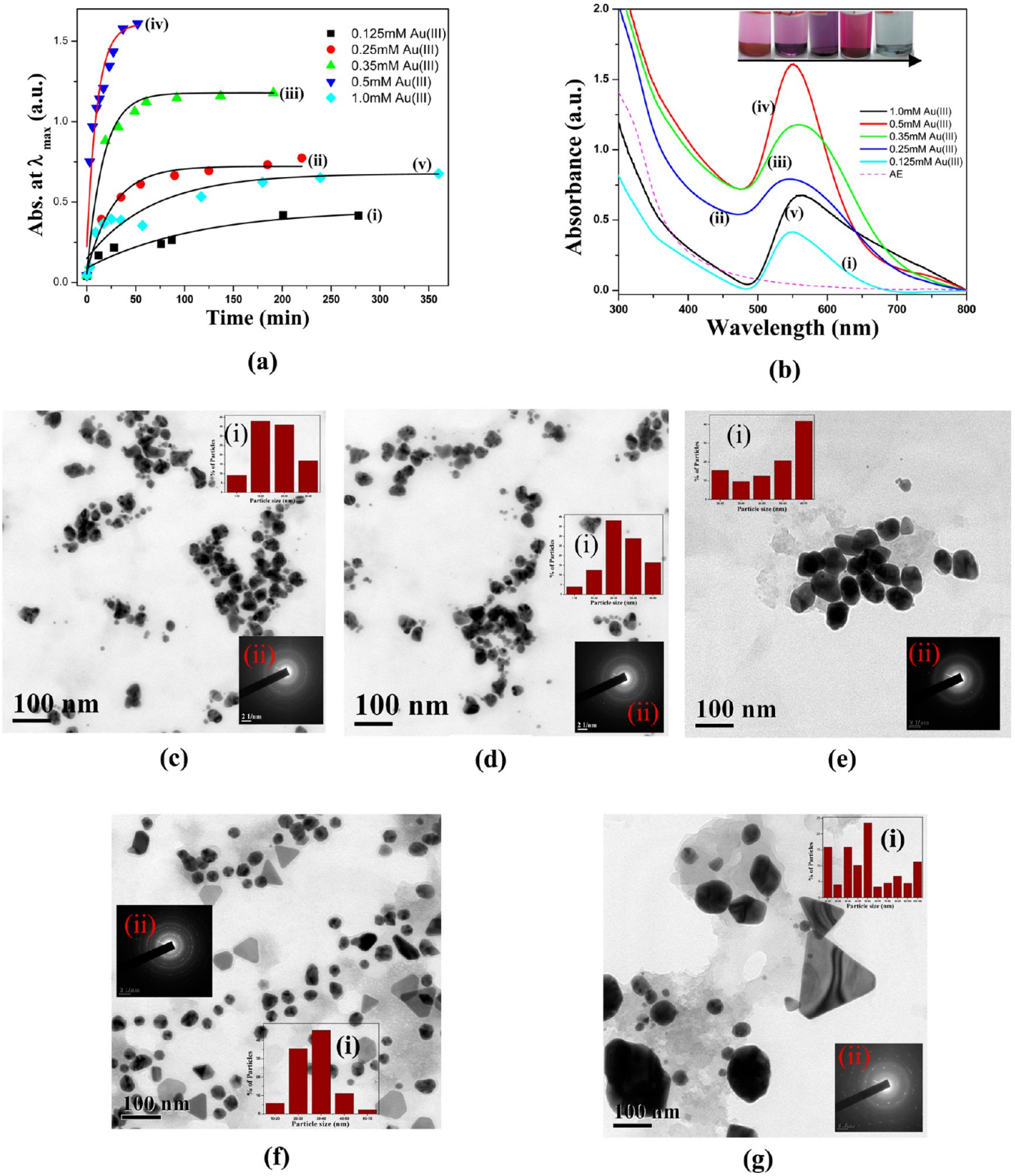

Figure 2. [a(i–v)] show the change in peak absorbance and peak absorption wavelength with time for Au NPs synthesized by 0.125, 0.25, 0.35, 0.5, and 1.0 mM Au (III) ion concentration, respectively, using 400 μg mL^{-1} of GAE at pH 7 and 50 °C. [b(i–v)] are corresponding UV–vis spectra of Au NPs at time of saturation. Broken line in (b) represents the absorbance curve of the reaction medium in the absence of Au (III) ions. Inset of (b) shows the color of the corresponding Au NPs solutions. TEM images show Au NPs prepared by different concentrations of Au (III) ion: 0.125 mM (c), 0.25 mM (d), 0.35 mM (e), 0.5 mM (f), and 1.0 mM (g). Insets (i) and (ii) show TEM images of corresponding particle size distribution histograms and SAED patterns of Au NPs, respectively.

Folin–Ciocalteu reagent according to the method of McDonald et al.[12]

Method of Controlled Synthesis of Au NPs Using AE as Green Multifunctional Agent. In general, the synthesis of Au NPs

was initiated by the addition of 100 μL of a 0.05 M aqueous solution of $HAuCl_4$ to 10 mL of an aqueous solution of GAE (400 μg mL^{-1}) so that the final Au (III) ion concentration in the reaction mixture became 0.5 mM. The reaction mixture was stirred continuously at 50 °C, whereby a pink coloration was developed within 3 min indicating the onset of formation of Au NPs. The progress of the reaction was monitored by measuring the absorbance of the reaction mixture at regular intervals of time. The absorption peak is assigned to the surface plasmon resonance (SPR) band of Au NPs, which arises due to coherent oscillation of the conduction band electrons induced by the interaction with an electromagnetic field.[13]

From our previous studies, it is evident that bioprocess parameters, for example, temperature, pH, precursor metal ion, and plant extract (GMA) concentrations, have prominent roles in the fine-tuning of the morphology of metal NPs synthesized by biogenic routes.[14−16] Here, we have done a systematic study on the effect of these bioprocess parameters in controlling the morphology of the Au NPs synthesized by the present route.

We have also synthesized Au NPs by AE at various temperatures (30, 50, 65, and 85 °C) and pH values (5, 7, 10, and 12) to note the temperature- and pH-dependency of this method. We have also optimized the concentrations of GAE and Au (III) ions through a series of trials. The effect of Au (III) ion concentration (0.125, 0.25, 0.35, 0.5, and 1.0 mM) was studied at neutral pH and 50 °C, whereas the role of GAE concentration (200, 300, and 400 μg mL^{-1}) was also studied at neutral pH and 50 °C using 100 μL of 0.05 M $HAuCl_4$ (final concentration in reaction mixture was 0.5 mM). In each case, the progress of the reaction was monitored by measuring the absorbance of the reaction mixture at regular intervals of time.

Method of Au NPs Synthesis by Quercetin and Quercetin-3-glucoside, the Active Components Present in AE of *Murraya koenigii* Spreng. Leaves. The synthesis of Au NPs was initiated by the addition of 100 μL of a 0.05 M aqueous solution of $HAuCl_4$ to 10 mL of a 0.1 mM aqueous solution of quercetin so that the final Au (III) ion concentration became 0.5 mM. The reaction mixture was stirred continuously at 50 °C and at pH ∼10. Development of pink coloration indicated the formation of Au NPs. The SPR band of the Au NPs that formed appeared at 522 nm. A similar process was repeated with 0.075 mM aqueous solution of quercetin-3-glucoside, while other reaction conditions were kept unchanged. In this case, the SPR band of Au NPs appeared at 551 nm.

RESULTS AND DISCUSSION

Formation and Growth of Au NPs Synthesized by AE as Green Multifunctional Agent. Figure 1(a) shows the results of the reaction between Au (III) ions and the aqueous solution of GAE (400 μg mL^{-1}) at neutral pH as a function of time of the reaction. The broken curve represents the absorption spectrum of the aqueous solution of GAE at t = 0, i.e., at the instant of addition of Au (III) ion. Upon stirring at 50 °C for 3 min, the Au SPR band appeared at 551 nm and steadily increased in intensity as a function of time. Finally, a saturation is observed at long times, i.e., at $t \geq 52$ min [inset (ii), Figure 1(a)]. Au NPs exhibit a pink/ruby red color in water as shown in inset (i) of Figure 1(a)].

Controlled Synthesis of Au NPs Using AE as Green Multifunctional Agent. *Effect of AE Concentration on Au NPs Synthesis.* We have also performed the same experiment by varying the GAE concentration (300 and 200 μg mL^{-1}) using 100 μL of 0.05 M $HAuCl_4$ at neutral pH and 50 °C. It is interesting to note that extract concentration has a prominent role on the shape and size of the synthesized Au NPs.

A broad SPR band of Au NPs was observed at around 543 nm after 17 min of continuous stirring and heating at 50 °C when the GAE concentration was 300 μg mL^{-1}. Here also the progress of the reaction was monitored by measuring the absorbance of the reaction mixture at regular intervals of time. The absorbance steadily built up with time leading to saturation at long times, i.e., at $t \geq 152$ min [Figure 1(b)].

When the extract concentration was 200 μg mL^{-1}, a broad SPR band of Au NPs was observed at 533 nm with a hump at 615 nm after 25 min of continuous stirring and heating at 50 °C. The absorbance steadily built up with time leading to saturation at long times, i.e., at $t \geq 275$ min [Figure 1(c)].

It is evident from Figure 1(a−c) that the sharpness of the SPR band of Au NPs strongly depends on the GAE concentration, while the SPR bandwidth increases with an decrease in the concentration of GAE [Figure 1(b) and (c)]. The broader nature of SPR bands obtained at lower concentration levels of GMA may be due to the formation of larger-sized anisotropic Au NPs.[17]

This was further confirmed from the corresponding TEM images [Figure 1(a.I−c.I)].

When GAE concentration was 400 μg mL^{-1}, the size of the Au NPs varied within 20−40 nm [inset (i), Figure 1(a.I). But it is interesting to note that although most of the particles appeared spheroidal, there are quite a few with a pronounced anisotropic morphology, like triangular, hexagonal, and nanorods [Figure 1(a.I)]. At lower concentration of GAE (300 μg mL^{-1}), particle size distribution is much broader (10−80 nm) [inset (i), Figure 1(b.I)]. Most of the particles appear spheroidal, but in a few cases, the NPs form small aggregations [Figure 1(b.I)]. But when the concentration of GAE was further decreased to 200 μg mL^{-1} keeping all the other conditions (pH, temperature, and metal ion concentration) fixed, the tendency of larger particles with occasional aggregation of the smaller particles was observed [Figure 1(c.I)]. This anisotropic morphology of the particles at lower concentration can be correlated with the appearance of a broader SPR band shown in Figure 1(a−c).

In all the three cases, SAED patterns [insets (ii) of Figure 1 (a.I−c.I)] denoted bright circular spots indicating the crystalline nature of synthesized Au NPs. Moreover, in all the cases, elemental Au peaks signals (at 2 and 9.7 keV) were found in energy dispersive X-ray analysis (EDX) data (Figure S1, Supporting Information) with a strong signal for Cu (at 8 keV), which may be due to the Cu in Cu grid used.

Effect of Au (III) Ion Concentration on Au NPs Synthesis. We examined the effect of metal ion concentrations (0.125, 0.25, 0.35, 0.5, and 1.0 mM) on the formation and growth of Au NPs at neutral pH and 50 °C, keeping the concentration of the multifunctional agent GAE in the range of 400 μg mL^{-1}.

At [Au (III)] = 0.125 mM, a nearly sharp but asymmetric SPR band was observed at around 549 nm after 12 min of continuous heating and stirring at 50 °C. Moreover, the absorbance at 549 nm steadily built up with time leading to saturation at long times, i.e., at $t \geq 278$ min [Figure 2(a)(i) and (b)(i)].

When [Au (III)] = 0.25 mM, a broad SPR band appeared at 547 nm after 10 min of continuous stirring and heating at 50 °C. In this case, too, absorbance of the reaction mixture at 547 nm steadily built up with time, and saturation was reached at long times, i.e., at $t \geq 220$ min [Figure 2 (a)(ii) and (b)(ii)].

Similar trends were observed when [Au (III)] = 0.35 mM. However, in this case, the SPR band (relatively sharper and symmetrical than the previous ones) was obtained at 558 nm after 8 min of continuous stirring and heating at 50 °C. The saturation limit was observed at long times, i.e., at $t \geq 191$ min [Figure 2(a)(iii) and (b)(iii)].

Table 1. Role of Bioprocess Parameters in Controlling Shape and Size of Au NPs Synthesized by *Murraya koenegii* Spreng. Leaf Extract as Green Multifunctional Agent

bioprocess parameters		rate constant (min^{-1})	morphology of Au NPs synthesized	remarks
(a) conc. of green multifunctional agent (GMA) ($\mu g\ mL^{-1}$)	400	0.094	Spheroidal Au NPs were formed along with a few particles with pronounced anisotropic morphology.	With the decrease in GMA conc., rate of Au NPs formation was found to be drastically reduced accompanied with visible change in shape and size of synthesized Au NPs.
	300	0.072	Most of the particles appeared spheroidal along with few small aggregations.	
	200	0.024	Larger particles with occasional aggregation were prominent.	
(b) conc. of precursor metal ion [Au (III)] (mM)	0.125	0.009	Anisotropic Au NPs were formed.	It is interesting to note that with an increase in Au (III) ion conc., the rate of the Au NPs formation increased for a fixed conc. of the multifunctional agent at neutral pH and 50 °C. But this was found to be valid up to an optimum conc. of Au (III) ions, i.e., in our case, 0.5 mM. Moreover, precursor metal ion conc. plays a vital role in controlling the morphology of the synthesized Au NPs.
	0.25	0.037	Similar anisotropic NPs formed but with larger size.	
	0.35	0.059	Mostly spherical Au NPs were observed along with few anisotropic NPs.	
	0.5	0.094	Au NPs were mostly spherical and well separated. But some larger particles with definite geometrical shapes were also prominent.	
	1.0	0.019	Larger anisotropic Au NPs were formed with occasional aggregation.	
(c) temp (°C)	30	0.011	Spherical Au NPs were formed with mostly uniform size distribution.	Temperature played a prominent role in controlling shape and size of Au NPs synthesized by the present method. The rate of formation of Au NPs was found to be proportional to the temperature. With the increase in temperature, along with spherical particles, other interesting geometrical shapes were also observed, especially 85 °C. But no prominent temperature effect on the growth kinetics of synthesized Au NPs was observed beyond 85 °C.
	50	0.094	Along with spherical Au NPs, particles with interesting regular geometrical shapes were also noticed. But size of the particles was mostly uniform.	
	65	0.124	Au NPs synthesized were found to be well separated and with definite geometrical shapes. But a wide range of size variation was also prominent.	
	85	0.226	Together with spheroid Au NPs, the nanorods, nanowedges and nanoprisms along with various regular geometrical shapes, i.e., triangles, hexagons, squares, and trapezoids, were abundant.	
(d) pH of reaction medium	5	0.023	Abundance of spherical Au NPs was diminished, while other regular geometrical shapes became predominant.	Visible change of morphology of Au NPs was observed with a change in pH. Optimum result was obtained at pH 7. At pH 7, the rate of formation of Au NPs was found to be the fastest. Rate of formation of Au NPs abruptly slowed at pH 5, and below pH 5, Au NPs could not be synthesized when we further lowered the pH of the reaction medium.
	7	0.094	Mostly spherical Au NPs (along with a very few anisotropic particles) having uniform size distribution were noticed.	
	10	0.031	Particles formed in this case have more wide range of size distribution. Formation of spherical particles was almost rare. Au NPs of hexagonal shape were predominant.	
	12	3.7×10^{-06} very slow	Au NPs formed were mostly spherical, and abundance of smaller particles was noticed.	

We also got similar results with [Au (III)] = 0.5 mM as discussed as earlier. It is interesting to note that at this concentration level of Au (III) ions, the optimum result was obtained with a perfectly symmetrical and narrow SPR band (at 551 nm) after 3 min under the same reaction condition. Moreover, the saturation point is reached faster, unlike the earlier three cases [Figure 2(a)(iv) and (b)(iv)].

But when the Au (III) concentration was increased to 1.0 mM, a drastic change in the corresponding SPR band (broad and unsymmetrical in nature and at 563 nm) was observed. Intensity of the SPR band is reduced. But in this case, also formation of Au NPs started after 3 min of continuous stirring and heating at 50 °C. The saturation of the SPR absorbance was reached at very long times, i.e., at $t \geq 360$ min [Figure 2(a)(v) and (b)(v)]. Insets of Figure 2(b) indicate that visual color changes (from pink to deep pink-red to light blue) occurred with an increase in the concentration of metal ion from 0.125 to 1.0 mM.

It is interesting to observe that with an increase in Au (III) ion concentration, the rate of the Au NPs formation increased for a fixed concentration of the multifunctional agent at neutral pH and 50 °C. But this was found to be valid up to a limiting concentration of Au (III) ions, i.e., in our case 0.5 mM, at the above-mentioned reaction condition. The formation and

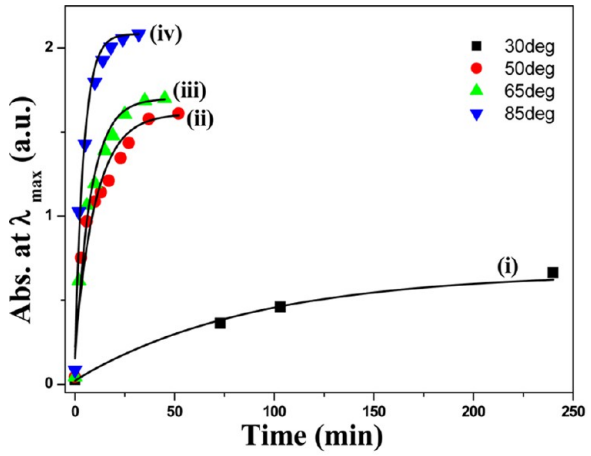

(a)

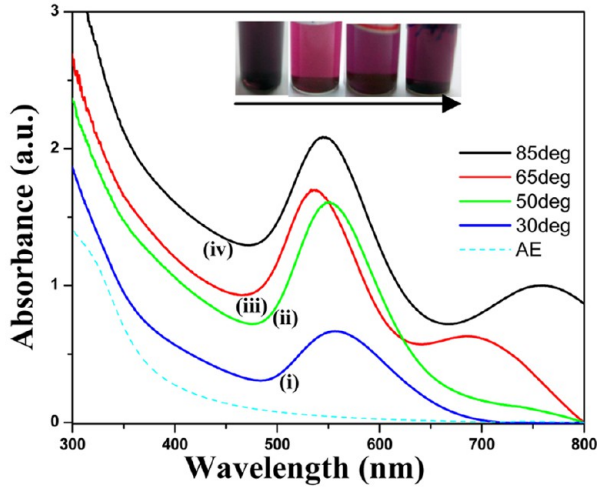

(b)

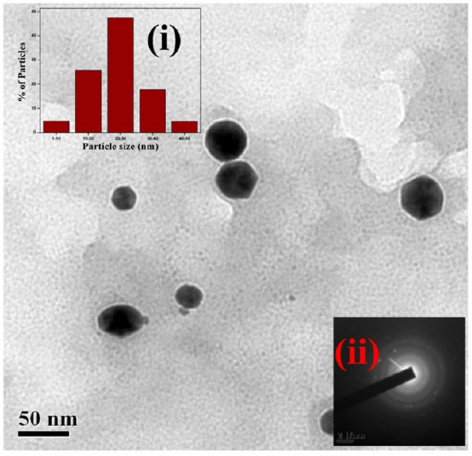

(c)

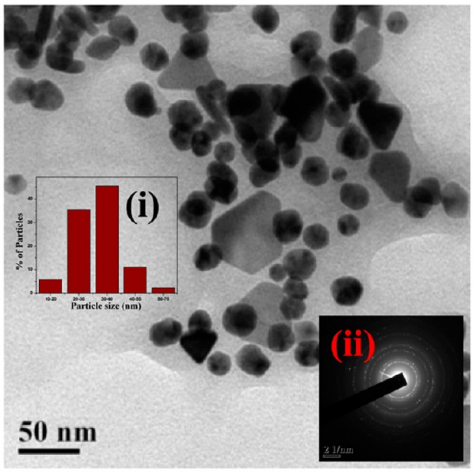

(d)

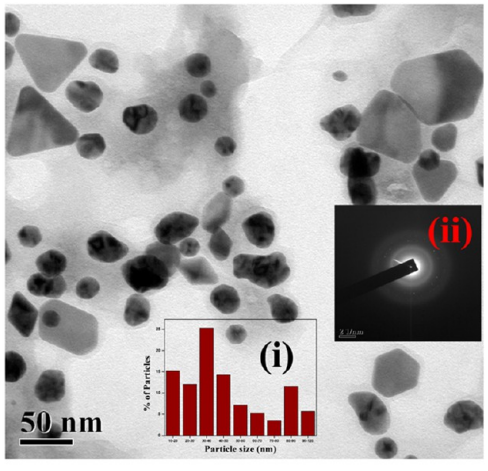

(e)

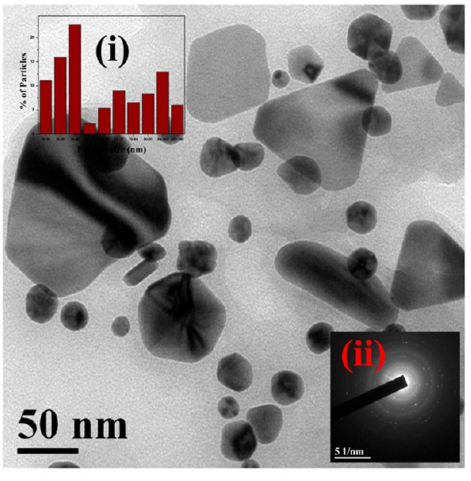

(f)

Figure 3. [a(i–iv)] show the change in peak absorbance maxima and peak absorption wavelength with time for Au NPs synthesized at 30, 50, 65, and 85 °C using 400 μg mL^{-1} of GAE and a 0.5 mM Au (III) ion concentration at pH 7. [b(i–iv)] show corresponding UV–vis spectra of Au NPs at time of saturation. Broken line in (b) represents the absorbance curve of the reaction medium in the absence of Au (III) ions. Inset of (b) shows the color of the corresponding Au NPs solutions. TEM images show Au NPs prepared at different temperatures: 30 °C (c), 50 °C (d), 65 °C (e), and 85 °C (f). Insets (i) and (ii) show TEM images of corresponding particle size distribution histograms and SAED patterns of Au NPs, respectively.

dx.doi.org/10.1021/sc400562w | ACS Sustainable Chem. Eng. 2014, 2, 652–664

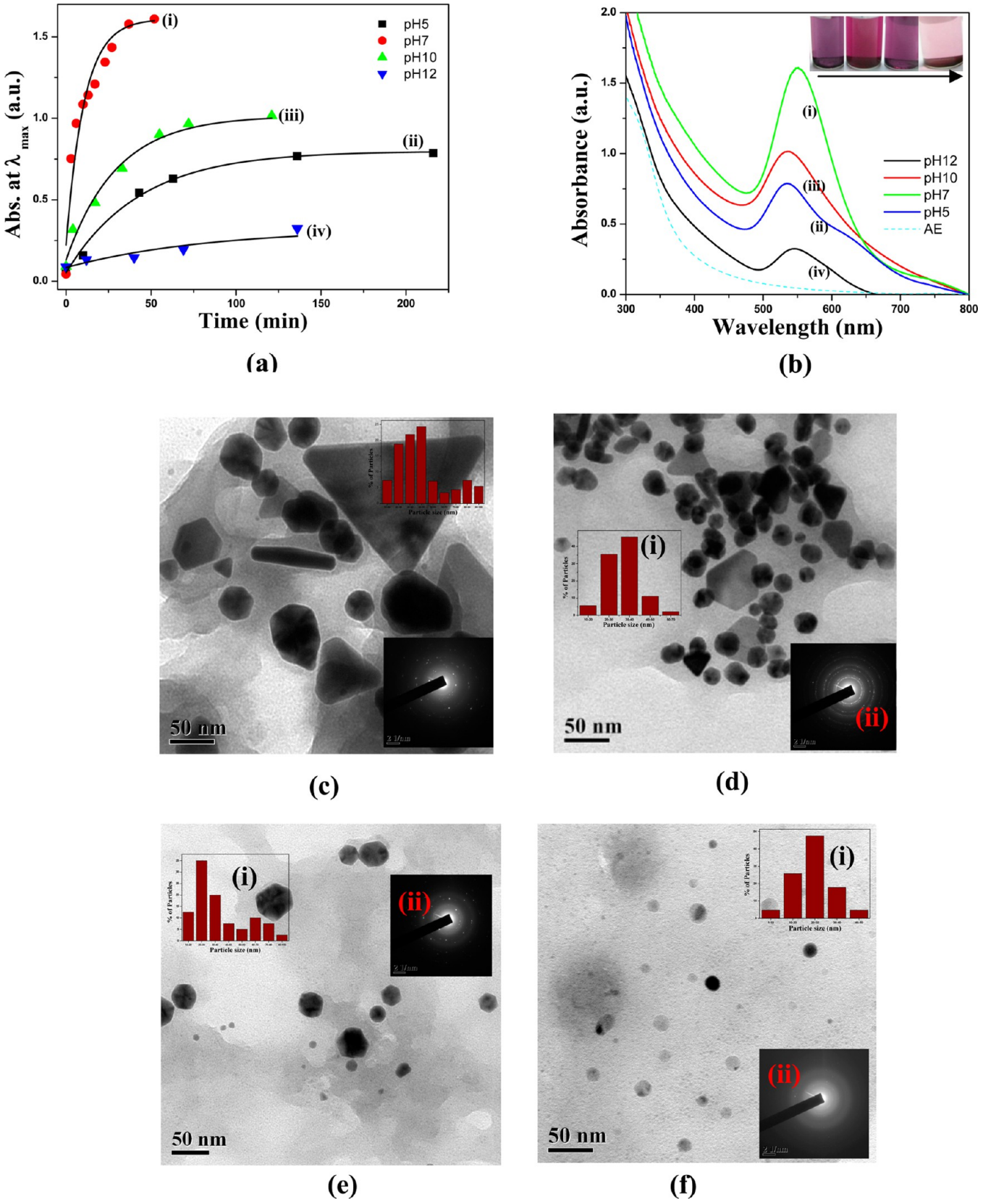

Figure 4. [a(i–iv)] show the change in peak absorbance maxima and peak absorption wavelength with time for Au NPs synthesized at pH 5, 7, 10, and 12, respectively, using 400 μg mL^{-1} of GAE at 50 °C and a 0.5 mM Au (III) ion. [b(i–iv)] show corresponding UV–vis spectra of Au NPs at time of saturation. Broken line in (b) represents the absorbance curve of the reaction medium in the absence of Au (III) ions. Inset of (b) shows the color of the corresponding Au NPs solutions. TEM images show Au NPs prepared at different pH: 5 (c), 7 (d), 10 (e), and 12 (f). Insets (i) and (ii) show TEM images of corresponding particle size distribution histograms and SAED patterns of Au NPs, respectively.

dx.doi.org/10.1021/sc400562w | ACS Sustainable Chem. Eng. 2014, 2, 652–664

growth rate of Au NPs were not enhanced beyond this concentration level (Table 1).

Interesting features were observed in the corresponding UV−visible spectra [Figure 2(b)(i−v)]. The SPR bandwidth became narrower, and absorption intensity increased with an increase in Au (III) ion concentration from 0.125 to 0.5 mM. But a broader SPR band with low intensity was noticed for the 1.0 mM Au (III) ion concentration. The appearance of a broad SPR band for Au NPs may be due to the formation of anisotropic NPs.[18] This was further confirmed from TEM images [Figure 2(c−g)].When the Au (III) ion concentration was increased from 0.25 to 0.35 mM, sharpness of the SPR band was not significantly changed, but a red shift was observed [Figure 2(b)(ii−iii)]. This red shift in the SPR band may be originated due to the formation of larger-sized Au NPs, which was further evidenced from TEM images of the corresponding systems [Figure 2(c−g)].[19] Again a slight blue shift of the sharper SPR band was noticed for the 0.5 mM Au (III) concentration [Figure 2(b)(iv)]. The TEM image revealed that in this case the particles were smaller in size, mostly spherical and well separated, and at the same time, some larger particles with definite geometrical shapes were also noticed [Figure 2(f)]. Large anisotropic particles were observed for the 1 mM Au (III) concentration [Figure 2(g)]. This observation is nicely correlated with the appearance of a broad but asymmetric SPR band in its UV−visible spectra [Figure 2(b)(v)].

Effect of Reaction Temperature on Au NPs Synthesis. The effect of temperature (at 30, 50, 65, and 85 °C) was studied using GAE having a concentration of 400 μg mL^{-1} and final metal precursor ion concentration of 0.5 mM at neutral pH.

At 30 °C, the rate of formation of Au NPs was found to be slowest (Table 1). Onset of Au NPs formation was noticed after 70 min of continuous stirring of the reaction mixture at this temperature, and the SPR band appeared at 556 nm. We observed the growth the absorbance curve at regular intervals of time, and a saturation is observed at long times, i.e., at $t \geq 240$ min [Figure 3(a)(i) and (b)(i)]. Spherical particles with mostly uniform size distribution (average size ∼30 nm) were found as shown in the TEM image [Figure 3(c)].

But when the same procedure was repeated at 50 °C, the Au NPs formation occurred almost instantaneously, i.e., within 3 min (Table 1). In this case, the Au SPR band appeared at 551 nm and steadily increased in intensity as a function of time. Finally, a saturation was observed at long times, i.e., at $t \geq 52$ min [Figure 3 (a)(ii) and (b)(ii)]. At this temperature in addition to spherical morphology, particles with other interesting geometrical shapes were also noticed. In this case, the sizes of the particles were mostly uniform. Moreover, the particles were closely spaced as evidenced in the corresponding TEM image [Figure 3(d)].

A more interesting feature was observed when the temperature was further raised to 65 °C, keeping all the reaction conditions unchanged. Like the earlier case, here also Au NPs formed at a faster rate (Table 1). The nature of the absorbance curve was totally different as shown in Figure 3(b)(iii). In this case, a double-humped curve was observed with the main peak at 537 nm and a shoulder at 688 nm [Figure 3(b)(iii)]. Both of these two absorbance bands rapidly grew with time, and a saturation was observed within 45 min [Figure 3(a)(iii) and (b)(iii)]. When we have repeated our experiment at 85 °C, the Au NPs formation occurred almost instantaneously (Table 1). But in this case, the nature of the absorbance curve was slightly different from the earlier one [Figure 3(b)(iv)]. Although, a double-humped curve was also observed here, the main peak (at 544 nm) was found to be sharper and a red-shifted broad shoulder at 761 nm was noticed, which grew with time, and a saturation was observed within 32 min [Figure 3(a)(iv) and (b)(iv)]. The color of the Au NPs solution at different temperatures did not change prominently [inset, Figure 3(b)].

The formation of two absorption bands at longer and shorter wavelengths is due to the longitudinal and transverse surface plasmon oscillation, respectively.[20] This phenomenon is actually related to the anisotropy of the metal NPs formed .[21,22] We have performed the TEM studies of the Au NPs formed at 65 and 85 °C [Figure 3(e) and (f), respectively]. When the temperature was 65 °C, the majority of the particles were found to be the average size of 30 nm, but a wide range of size variation was also prominent as evidenced from the particle size distribution diagram [inset (i), Figure 3(c)]. In this time, the particles were found to be well separated and with definite geometrical shapes; for example, triangles were clearly visible [Figure 3(e)].

At 85 °C, a wide range of size distributions of the Au NPs was observed [inset (i), Figure 3(f)]. But unlike previous temperatures, in the present case together with spheroids, the nanorods, nanowedges, and nanoprisms of various regular geometrical shapes, such as triangles, hexagons, squares, and trapezoids, were plentiful [Figure 3(f)].

We have also repeated our experiments at higher temperatures, but no temperature effect on the growth kinetics of synthesized Au NPs was observed beyond 85 °C.

In summary, we can say that up to a certain level temperature played a prominent role in controlling shape and size of Au NPs synthesized by an aqueous solution of GAE. With an increase in temperature, along with spherical particles, nanorods as well as nanoprisms of triangular, pentagonal, and trapezoidal cross-sections were found to be predominant, especially 85 °C.

Effect of pH on Au NPs Synthesis. To note the effect of pH on controlling the shape and size of Au NPs synthesized by the present protocol, we have repeated our experiments at various pH using the same concentration of aqueous solution of GAE (i.e., 400 μg mL^{-1}) and final metal precursor ion concentration 0.5 mM and at 50 °C. We have found that like GAE and metal precursor ion concentrations and also temperature, control of pH of the reaction medium may be helpful to synthesize Au NPs with fine-tuned structures using this biogenic route.

At pH 7, the rate of formation of Au NPs was found to be the fastest (Table 1). Formation of Au NPs started within 3 min of stirring of the reaction mixture at 50 °C, which was indicated by the appearance of a perfectly symmetrical and sharp SPR band of Au NPs at 551 nm [Figure 4(b)(i)]. Absorbance at 551 nm steadily increased in intensity with time, and finally, a saturation was observed at long times, i.e., at $t \geq 52$ min [Figure 4(a)(i) and (b)(i)]. Mostly spherical particles (along with a very few anisotropic particles) having uniform size distribution were noticed in the TEM image [Figure 4(d)].

When the pH of the reaction mixture was decreased to 5, the rate of formation of Au NPs abruptly slowed down (Table 1). After 40 min of continuous stirring of the reaction mixture at 50 °C, onset of formation of Au NPs was noticed. In this case, a broader SPR band appeared at 533 nm along with a small hump at 617 nm [Figure 4(b)(ii)]. We studied the growth of the absorbance curve at regular intervals of time, and a saturation is observed at long times, i.e., at $t \geq 216$ min [Figure 4(a)(ii) and (b)(ii)].

But fascinating morphology of the Au NPs was observed at this pH. Particles formed had a wide range of size distribution [inset (i), Figure 4 (c)], but abundance of spherical-shaped particles was noticeably diminished [Figure 4 (c)].Together with spheroid Au NPs, the nanowedges and nanoprisms and other regular geometrical shapes, such as triangles, hexagons, squares, and trapezoids, are clearly visible in the TEM image [Figure 4(c)].

Au NPs could not be synthesized by AE as a green multifunctional agent when we further lowered the pH of the reaction medium. The decrease in the Au (III) ion reduction rate observed at pH 5 may be attributed to the fact that redox behavior of the active components (e.g., polyphenols and flavonoids) present in this GMA is highly dependent on pH of the reaction medium.[23−25] This is further confirmed from the CV studies of AE of *Murraya koenigii* Spreng. leaves at different pH values (Figure S2, Supporting Information). These active components actually play a dual role of reducing and stabilizing agents for the synthesis of Au NPs by AE of *Murraya koenigii* Spreng. leaves. In strongly acidic pH, the reducing functional groups of the biomolecules responsible for the reduction of Au (III) to Au (0) are blocked or deactivated,[23,24] which is also evidenced from the reduction potential values of AE of *Murraya koenigii* Spreng. leaves shown in Figure S2 of the Supporting Information. Hence, the nucleation and growth of Au NPs were drastically slowed down.

We have also repeated the experiment at pH 10. In this case, the rate of formation of Au NPs again decreased, but it still higher than the rate observed at pH 5 (Table 1). Onset of formation of Au NPs was indicated by the appearance of a broader SPR band at 537 nm within 5 min of stirring of the reaction mixture at 50 °C, and a saturation was observed within 121 min [Figure 4(a)(iii) and (b)(iii)]. Particles formed at this pH had more wide range of size distribution unlike the previous two pH values as shown in inset (ii) of Figure 4(e). It is noticeable that at this pH value formation of spherical particles was almost rare. Moreover, Au NPs of hexagonal shape predominated as evidenced in the corresponding TEM image [Figure 4(e)].

We have again increased the pH of the reaction medium to 12. In this case the rate of formation of Au NPs became very slow (Table 1). Formation of Au NPs started within 69 min of continuous stirring, which was indicated by the appearance of a broad and very low intensity SPR band at 547 nm, and a saturation was observed after 136 min [Figure 4(a)(iv) and (b)(iv)]. Particles formed in this case had uniform size distribution as shown in inset (i) of Figure 4(f). It is interesting to observe that although the rate of formation of NPs was found to be very slow, particles formed were mostly smaller and spherical along with very few larger spherical particles as shown in the corresponding TEM image [Figure 4(f)].

When we further increased the pH, the formation of Au NPs by this route almost stopped.

XRD analyses were carried out to study the crystal structure of Au NPs synthesized at different pH ranges of the reaction medium as shown in Figure S3(a) of the Supporting Information. In all the cases, the presence of four lattice planes, viz., (111), (200), (220), and (311), of fcc Au NPs leading to the diffraction peaks at almost 38.3, 44.3, 64.7, and 77.6°, respectively, were observed in the XRD pattern [Figure S3(a), Supporting Information]. These results indicate the formation of Au NPs[26] (metallic gold, JCPDS 04-0784) at different pH values of the reaction medium.

Moreover, these results are in accordance with SAED patterns shown in inset (ii) of the corresponding TEM images. Energy dispersive X-ray study (EDX) studies of the Au NPs synthesized at different pH values of the reaction medium also confirmed the presence of elemental Au in the synthesized NPs [Figure S3(b), Supporting Information]. EDX spectra of Au NPs synthesized at different pH values were found to be identical, and clear signals for elemental gold with a strong signal for copper (Cu) were observed, which may be due to Cu in the Cu grid used for the experiment [Figure S3(b), Supporting Information].

Growth Kinetics of Controlled Synthesis of Au NPs Using AE. The absorbance spectra in all the cases exhibit common features, for example, absorbance initially increased significantly became steady over a longer period of time and then reached an almost constant value after several minutes. This phenomenon may also reflect the formation of new NPs by the conversion of smaller NPs to larger ones or vice versa or the alteration of NP shape and morphological characteristics of Au NPs.

The variation of absorbance maxima with time are shown in the insets (ii) of Figures 1(a−c), 2 (a), 3 (a), and 4 (a). All these plots (absorbance maxima vs time) were best fitted to the following first-order exponential growth function

$$A\ (\text{absorbance}) = A_0 \text{X}\ \exp(kt)$$

The first-order rate constants for the formation of Au NPs by the processes discussed in the present paper are listed in Table 1.

As shown in Table 1, the increase in the rate constant with an increase in temperature demonstrates that this synthesis process of Au NPs using AE is an activated process. Using a more complicated fitting function, such as a polyexponential or stretched exponential, did not provide any additional information. A simple first-order exponential growth was useful in all cases, suggesting that the underlying molecular processes in all cases are similar.

Identification of Multifunctional Biomolecules Involved in Synthesis of Au NPs by AE of *Murraya koenigii* Spreng. Leaves. We have performed cyclic voltammetry (CV) studies AE of *Murraya koenigii* Spreng. leaves to determine its redox behavior (Figure S2, Supporting Information). The appearance of a broad anodic peak may be due to several similar types of chemical constituents present in the extracts.[14]

For further identification of the active chemical constituents that control the redox behavior of AE of *Murraya koenigii* Spreng. leaves, we have determined its total polyphenols and flavonoid contents. During our previous studies, we have found that the main active constituents in most of the plant-based multifunctional agents are polyphenols and flavonoids that have strong roles in the synthesis and stabilization of metal NPs.[15,16,27]

In the present case, total polyphenol and flavonoid contents of AE of *Murraya koenigii* Spreng. leaves were found to be 81.9 mg Gallic acid equivalent g^{-1} and 39.98 mg of duercetin g^{-1}, respectively. Polyphenols and flavonoids are well known for their antioxidant activity (which is the indirect measure of their reducing activity).[9,28] It is probable that these types of constituent molecules may impart a specific type of reducing characteristic to the AE of *Murraya koenigii* Spreng. leaves that was exploited for the synthesis of Au NPs by the reduction of Au (III) ions in the present case.

To confirm these facts, we have performed FT-IR spectroscopic measurements of GAE before and after the Au NPs synthesis (Figure S4, Supporting Information). Prominent IR bands of GAE appearing within the range of 1800−1000 cm^{-1} are 1696, 1628, 1452, 1371, 1302, 1158, and 1089 cm^{-1}. Among these, the peaks at 1696, 1628, 1371, and 1158 cm^{-1} are associated with the stretching vibration for −C═C−C═O, −C═C− [(in-ring) aromatic], C−O (ester, ether), and C−O (polyol), respectively. So these are the IR spectroscopic evidence for the presence of polyphenol, polyhydroxy flavonoid, and the glycoside type of compounds present in this extract.[27−29]

To further identify these flavonoids and polyphenols, we have performed HPLC of AE of *Murraya koenigii* Spreng. leaves. From this study, it is evident that quercetin and quercetin-3-glucoside were present in the extract that was in accordance with literature data.[30] Retention times of quercetin and quercetin-3-glucoside were found to be 15.926 and 5.609 min, respectively [Figure S5(b) and (c), Supporting Information]. When HPLC was performed for AE of *Murraya koenigii* Spreng. leaves, two peaks at 16.614 and 5.609 min were found [Figure S5(a), Supporting Information]. These were comparable to the retention peaks for quercetin and quercetin-3-glucoside. HPLC results confirmed the presence of polyhydroxy flavonoids and flavonoids glycoside (polyols) that actually control the Au NPs synthesizing potential of these plant-based multifunctional agents.

It is evident that these chemical components of AE of *Murraya koenigii* Spreng. leaves are acting as the reducing agents and also as the stabilizing agents by adhering on the surface of the NPs formed, thereby preventing their aggregation and controlling the particle size. To understand this phenomenon, we have studied the thermal stability of the synthesized Au NPs using TGA.

The TGA plot of Au NPs synthesized by AE of *Murraya koenigii* Spreng. leaves (Figure S6, Supporting Information) indicates that there was an initial weight loss of 1.74% up to 150 °C. This may be due to the loss of water molecules present with Au NPs. Also, a steady weight loss of Au NPs powder was noticed within 150−655 °C. Total weight loss was found to be 27.41%. This may be explained by the fact that a surface desorption of an active component, for example, polyhydroxy flavonoids and flavonoids glycoside (polyols), present in the AE of *Murraya koenigii* Spreng. leaves occurred during TGA. Hence, these biomolecules played a vital role in the stabilization of these Au NPs.

Formation and Growth of Au NPs Synthesis by Quercetin and Quercetin-3-glucoside. Because our results provided strong evidence toward the presence of quercetin and quercetin-3-glucoside (which are polyhydroxy flavonoids and flavonoid glycosides type of compounds), we have also tested the Au NPs synthesis efficacy of these compounds. UV−vis absorption spectra showed the formation and growth of Au NPs by quercetin and quercetin-3-glucoside [Figure S7(a) and (b), Supporting Information, respectively], while TEM images of Au NPs formed by quercetin and quercetin-3-glucoside [Figure S7(c) and (d), Supporting Information, respectively] confirm the shape and size of the synthesized particles. Au NPs are predominantly spherical in shape and mostly uniform in size in both the cases.

It is evident that these compounds present in the extract may have a strong role in the formation and stabilization of Au NPs. Moreover it is interesting to note that a more homogeneous size and shape distribution of Au NPs were found in these two cases compared to the parent material, i.e., AE of *Murraya koenigii* Spreng. leaves. This is probably because of the fact that the later is a concoction of various naturally derived compounds in addition to quercetin and quercetin-3-glucoside that have different reducing and stabilizing activities leading to formation of particles of various different size and shape.

Fluorescence Study of Au NPs by AE of *Murraya koenigii* Spreng. Leaves. Fluorescence spectroscopic studies of an aqueous solution of GAE (of concentration 400 $\mu g\ mL^{-1}$) and the Au NPs solution synthesized by it at 50 °C and neutral pH were done at an excitation wavelength of 300 nm and are shown in Figure S8(a)(i) and (a)(ii) of the Supporting Information, respectively. A broad emission maxima was observed at ∼420 nm [Figure S8(a), Supporting Information]. After formation of Au NPs, a decrease in emission intensity was observed. This emission characteristic may be due to the attachment of the biomolecules present in the extract (mainly polyphenols) flavonoids (which have characteristic emissive nature) on the surface of Au NPs synthesized by the reduction of Au (III) ions followed by stabilization. This phenomenon may due to the close proximity of the emission spectra of several similar types of active species present in the Au NPs solution containing GAE, and this quenching of emission took place through energy transfer process.[31] This observation indicates that the components of AE of *Murraya koenigii* Spreng. leaves are acting as both reducing as well as stabilizing agents.

This is further proved from the fluorescence emission spectra of the Au NPs solution synthesized from active components of AE of *Murraya koenigii* Spreng. leaves, for example, quercetin and quercetin-3-glucoside [Figure S8(b)(i) and (ii), Supporting Information, respectively]. Moreover, this kind of study on the interaction between metal NPs and surface-adsorbed fluorescent groups is also a profoundly interesting issue in physicochemical investigations like energy transfer and near-field optical enhancement,[32] which have uncovered prospects of fabricating novel photonic devices.

Elucidation of a Probable Mechanistic Pathway. Understanding the mechanistic path of this type of green synthesis of metal NPs is highly essential for fine tuning these processes that will yield a range of metal NPs with tailor-made structural properties. Moreover, in most of the reported works,[8] the overwhelming emphasis was on the production of NPs itself, with little or no attention being paid to the mechanistic pathways of the synthesis process. Without any idea of the underlying chemical reactions and the reactants and stabilizers involved in it, a given synthetic method remains more of a vague empirical fact rather than a solid piece of scientific knowledge.

We have tried to determine a plausible mechanistic path for the present method. From the IR spectroscopic measurement, it is evident after reduction of Au (III) ions bythe aqueous extract of GAE that the bands at 1696, 1628, 1371, and 1158 cm^{-1}, which are associated with the stretching vibration for −C═C−C═O, −C═C− [(in-ring) aromatic], C−O (ester, ether), and C−O (polyol), respectively, totally disappeared, and new bands at 1731,1668, 1616, 1521, and 1421 cm^{-1} appeared (Figure S4, Supporting Information). This may be due to the fact that polyols (e.g., polyphenols, flavonoids, and glycosides) are actually responsible for the reduction of Au (III) ions, whereby they themselves get oxidized to an α,β-unsaturated

Scheme 1. Tentative Mechanism of Formation of Au NPs Synthesized by the Reduction of Au (III) Ions AE of *Murraya koenigii* Spreng. Leaves[27]

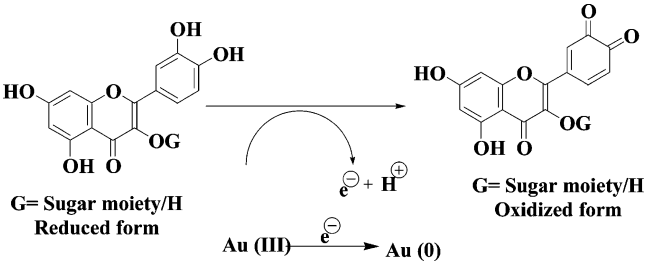

carbonyl group leading to the appearance of new peaks at 1668 cm^{-1}.[27]

On the basis of this observation, we have proposed a plausible mechanism as shown in Scheme 1.

There is a demand for development of reliable, cost-effective, and environment friendly protocols for the synthesis of metal NPs with finely tuned structures for technological applications. We have demonstrated that a naturally occurring plant source, i.e., leaves of *Murraya koenigii* Spreng., can play an important role in the formation and stabilization of Au NPs with various shapes and sizes with high monodispersity. Thus, our method is a promising green tool for the synthesis of Au NPs with tailor-made structural properties.

AE of *Murraya koenigii* Spreng. leaves was found to be rich in polyphenols, flavonoids, and glycosides.[9,28] In the present study, these compounds are acting as complex multifunctional green chemical reducing agents as well as stabilizing agents.

Moreover, the uniqueness of the present biogenic synthetic route is that simple experimental parameters like control of concentration of multifunctional agent and precursor metal ion and also pH and temperature can be effective in the synthesis of Au NPs with finely tuned structures.

We have also proposed a plausible mechanistic pathway for our synthetic method, which may aid in fine-tuning green chemical methods for the controlled synthesis of various metal NPs.

At the same time, our study on the interaction between Au NPs and surface-adsorbed fluorescent groups may also be helpful for physicochemical investigations like energy transfer and near-field optical enhancement.[33] This type of study may be extended and exploited in the future for fabricating novel photonic devices. Moreover, this study can be explored further in future for the surface modification of metal NPs, which is essential to understand and enhance the catalytic activity of metal NPs supported on various types of organic and inorganic moieties.[26]

■ ASSOCIATED CONTENT

Supporting Information

EDX profiles of Au NPs synthesized by aqueous solution of GAE of different concentration levels (400, 300 and 200 $\mu g\ mL^{-1}$) at pH 7 and 50 °C. Cyclic voltammetry of AE of *Murraya koenigii* Spreng. leaves. XRD patterns and EDX analyses of Au NPs synthesized by AE of *Murraya koenigii* Spreng. leaves at different pH ranges of the reaction medium and at 50 °C. FT-IR spectroscopic study of GAE of *Murraya koenigii* Spreng. leaves before and after the Au NPs synthesis. HPLC chromatograms of the aqueous extract of *Murraya koenigii* Spreng. leaves and its constituents quercetin and quercetin-3-glucoside. TGA plot of Au NPs synthesized using *Murraya koenigii* Spreng. leaves aqueous extract. UV−vis spectra and TEM images of Au NPs prepared by an aqueous solution of quercetin and quercetin-3-glucoside, respectively. Fluorescence emission spectra of Au NPs solution synthesized by quercetin and quercetin-3-glucoside and of an aqueous solution of quercetin and quercetin-3-glucoside. Fluorescence emission spectra of an aqueous solution of GAE (of concentration 400 $\mu g\ mL^{-1}$) and the Au NPs solution synthesized by it. This material is available free of charge via the Internet at http://pubs.acs.org.

■ AUTHOR INFORMATION

Corresponding Author

*E-mail: naznin.begum@visva-bharati.ac.in. Tel: +91 9434431810. Fax: +91 3463261526.

Notes

The authors declare no competing financial interest.

■ ACKNOWLEDGMENTS

We thank SERB-DST (Sanction No. SR/SO/BB-0007/2011, dated August 21, 2012, to N.A.B.) and CSIR, India [Sanction No. 01 (2504)/11/EMR-II) to N.A.B.] for their financial support. S.D. and M.N.A. are thankful to CSIR for their fellowship. S.B. and A.C. thank UGC for their fellowships (MANF and UGC-NET respectively). We thank the Department of Chemistry, Siksha Bhavana, Visva Bharati University, and its DST-FIST and UGC-SAP (Phase-II) programme for necessary infrastructural and instrumental facilities. We also acknowledge Professor S. Das in the Department of Metallurgical and Materials Engineering, IIT, Kharagpur-721302, and W.B. for use of the TEM facility.

■ REFERENCES

(1) Ba, H.; Rodríguez-Fernàndez, J.; Stefani, F. D.; Feldmann, J. Immobilization of gold nanoparticles on living cell membranes upon controlled lipid binding. *Nano Lett.* **2010**, *10* (8), 3006−3012.

(2) Chen, P. C.; Mwakwari, S. C.; Oyelere, A. K. Gold nanoparticles: From nanomedicine to nanosensing. *Nanotechnol., Sci. Appl.* **2008**, *1*, 45−66.

(3) Kumar, B.; Yadav, P. R.; Goel, H. C.; Rizvi, M. M. A. Recent developments in cancer therapy by the use of nanotechnology. *Digest J. Nanomater. Biostruct.* **2009**, *4* (1), 1−12.

(4) Thompson, M. J.; Bashford, D.; Noodleman, L.; Getzoff, E. D. Photoisomerization and proton transfer in photoactive yellow protein. *J. Am. Chem. Soc.* **2003**, *125* (27), 8186−8194.

(5) Sperling, R. A.; Gil, P. R.; Zhang, F.; Zanella, M.; Parak, W. J. Biological applications of gold nanoparticles. *Chem. Soc. Rev.* **2008**, *37* (9), 1896−1908.

(6) Mokari, T.; Habas, S. E.; Zhang, M.; Yang, P. Synthesis of lead chalcogenide alloy and core−shell nanowires. *Angew. Chem., Int. Ed.* **2008**, *47* (30), 5605−5608.

(7) Sànchez-Ramírez, J. F.; Pal, U.; Nolasco-Hernàndez, L.; Mendoza-Àlvarez, J.; Pescador-Rojas, J. A. Synthesis and optical properties of Au−Ag alloy nanoclusters with controlled composition. *J. Nanomater.* **2008**, *2008* (2008), 1−9.

(8) Alam, M. N.; Roy, N.; Mandal, D.; Begum, N. A. Green chemistry for nanochemistry: Exploring medicinal plants for the biogenic synthesis of metal NPs with fine-tuned properties. *RSC Adv.* **2013**, *3* (30), 11935−11956.

(9) Ningappa, M. B.; Dinesha, R.; Srinivas, L. Antioxidant and free radical scavenging activities of polyphenol-enriched curry leaf (*Murraya koenigii* L.) extracts. *Food Chem.* **2008**, *106* (2), 720−728.

(10) Philip, D. Biosynthesis of Au, Ag and Au−Ag nanoparticles using edible mushroom extract. *Spectrochim. Acta, Part A* **2009**, *73* (2), 374−381.
(11) Chang, C.; Yang, M.; Wen, H.; Chern, J. Estimation of total flavonoid content in propolis by two complementary colorimetric methods. *J. Food Drug Anal.* **2002**, *10* (3), 178−182.
(12) McDonald, S.; Prenzler, P. D.; Antolovich, M.; Robards, K. Phenolic content and antioxidant activity of olive extracts. *Food Chem.* **2001**, *73* (1), 73−84.
(13) Mulvaney, P. Surface plasmon spectroscopy of nanosized metal particles. *Langmuir* **1996**, *12* (3), 788−800.
(14) Mondal, S.; Roy, N.; Laskar, R. A.; Basu, S.; Mandal, D.; Begum, N. A. Biogenic synthesis of Au, Ag and bimetallic Au/Ag nanopaticles using mahogany (*Swietenia mahogany* JACQ.) leaf extract. *Colloids Surf., B* **2011**, *82* (2), 497−504.
(15) Roy, N.; Alam, M. N.; Mondal, S.; Sk, I.; Laskar, R. A.; Das, S.; Mandal, D.; Begum, N. A. Exploring Indian Rosewood as a promising biogenic tool for the synthesis of metal nanoparticles with tailor-made morphologies. *Process Biochem.* **2012**, *47* (9), 1371−1380.
(16) Roy, N.; Mondal, S.; Laskar, R. A.; Basu, S.; Mandal, D.; Begum, N. A. Biogenic synthesis of Au and Ag nanoparticles by Indian propolis and its constituents. *Colloids Surf., B* **2010**, *76* (1), 317−325.
(17) Bar, H.; Bhui, D. K.; Sahoo, G. P.; Sarkar, P.; De, S. P.; Misra, A. Green synthesis of silver nanoparticles using latex of *Jatropha curcas*. *Colloids Surf., A* **2009**, *339* (1−3), 134−139.
(18) Philip, D. Green synthesis of gold and silver nanoparticles using *Hibiscus rosasinensis*. *Phys. E* **2010**, *42* (5), 1417−1424.
(19) Mock, J. J.; Barbic, M.; Smith, D. R.; Schultz, D. A.; Schultz, S. Shape effects in plasmon resonance of individual colloidal silver nanoparticles. *J. Chem. Phys.* **2002**, *116* (15), 6755−6759.
(20) Hao, E.; Schatz, G. C.; Hupp, J. Synthesis and optical properties of anisotropic metal nanoparticles. *J. Fluoresc.* **2004**, *4* (4), 331−389.
(21) Link, S.; Wang, Z. L.; El-Sayed, M. A. Alloy formation of Au-silver nanoparticles and the dependence of the plasmon absorption on their composition. *J. Phys. Chem. B.* **1999**, *103* (18), 3529−3533.
(22) Jin, R.; Cao, Y. C.; Hao, E.; Metraux, G. S.; Schatz, G. C.; Mirkin, C. A. Controlling anisotropic nanoparticle growth through plasmon excitation. *Nature* **2003**, *425* (6957), 487−490.
(23) Ratasuk, N.; Nanny, M. A. Characterization and quantification of reversible redox sites in humic substances. *Environ. Sci. Technol.* **2007**, *41* (22), 7844−7850.
(24) Hernández-Montoya, V.; Alvarez, L. H.; Montes-Morán, M.; Cervantes, F. J. Reduction of quininone and non-quinone redox functional groups in different humic acid samples by *Geobacter sulfurreducens*. *Geoderma* **2012**, *183*−*184*, 25−31.
(25) Garg, D.; Muley, A.; Khare, N.; Marar, T. Comparative analysis of phytochemical profile and antioxidant activity of some Indian culinary herbs. *Res. J. Pharm., Biol. Chem. Sci.* **2012**, *3* (3), 845−854.
(26) Palashuddin, S. M.; Jana, C. K.; Chattopadhyay, A. A gold−carbon nanoparticle composite as an efficient catalyst for homocoupling reaction. *Chem. Commun.* **2013**, *49* (74), 8235−8237.
(27) Begum, N. A.; Mondal, S.; Basu, S.; Laskar, R. A.; Mandal, D. Biogenic synthesis of Au and Ag nanoparticles using aqueous solutions of black tea leaf extracts. *Colloids Surf., B* **2009**, *71* (1), 113−118.
(28) Shrestha, S. P.; Amano, Y.; Narukawa, Y.; Takeda, T. Nitric oxide production inhibitory activity of flavonoids contained in trunk exudates of *Dalbergia sissoo*. *J. Nat. Prod.* **2008**, *71* (1), 98−101.
(29) Reddy, R. V. N.; Reddy, N. P.; Khalivulla, S. I.; Reddy, M. V. P.; Gunasekar, D.; Blond, A.; Bodo, B. *O*-prenylated flavonoids from *Dalbergia sissoo*. *Phytochem. Lett.* **2008**, *1* (1), 23−26.
(30) Singh, A. P.; Wilson, T.; Luthria, D.; Freeman, M. R.; Scott, R. M.; Bilenker, D.; Shah, S.; Somasundaram, S.; Vorsa, N. LC-MS−MS characterisation of curry leaf flavonols and antioxidant activity. *Food Chem.* **2011**, *127* (4), 80−85.
(31) Bar, H.; Bhui, D. K.; Sahoo, G. P.; Sarkar, P.; Pyne, S.; Misra, A. Green synthesis of silver nanoparticles using seed extract of *Jatropha curcas*. *Colloids Surf., A* **2009**, *348* (1−3), 212−216.
(32) Dulkeith, E.; Morteani, A. C.; Niedereichholz, T.; Klar, T. A.; Feldmann, J. Fluorescence quenching of dye molecules near gold nanoparticles: Radiative and nonradiative effects. *Phys. Rev. Lett.* **2002**, *89* (20), 203002−1−203002−4.
(33) Ghoreishi, S. M.; Behpour, M.; Khayatkashani, M. Green synthesis of silver and gold nanoparticles using *Rosa damascena* and its primary application in electrochemistry. *Phys. E* **2011**, *44* (1), 97−104.